MOLECULAR AND CELLULAR BIOLOGY, Dec. 1994, p. 8259–8271
0270-7306/94/$04.00+0

Vol. 14, No. 12

MID1, a Novel *Saccharomyces cerevisiae* Gene Encoding a Plasma Membrane Protein, Is Required for Ca^{2+} Influx and Mating

HIDETOSHI IIDA,[1]* HIRO NAKAMURA,[1]† TOMOKO ONO,[1] MAKIKO S. OKUMURA,[1] AND YASUHIRO ANRAKU[1,2]

Division of Cell Proliferation, National Institute for Basic Biology, Okazaki 444,[1] and Department of Plant Sciences, Graduate School of Science, University of Tokyo, Tokyo 113,[2] Japan

Received 13 June 1994/Returned for modification 22 July 1994/Accepted 20 September 1994

By establishing a unique screening method, we have isolated yeast mutants that die only after differentiating into cells with a mating projection, and some of them are also defective in Ca^{2+} signaling. The mutants were classified into five complementation groups, one of which we studied extensively. This mutation defines a new gene, designated *MID1*, which encodes an N-glycosylated, integral plasma membrane protein with 548 amino acid residues. The *mid1-1* mutant has low Ca^{2+} uptake activity, loses viability after receiving mating pheromones, and escapes death when incubated with high concentrations of $CaCl_2$. The *MID1* gene is nonessential for vegetative growth. The efficiency of mating between *MAT*a *mid1-1* and *MAT*α *mid1-1* cells is low. These results demonstrate that *MID1* is required for Ca^{2+} influx and mating.

In cells of the yeast *Saccharomyces cerevisiae*, Ca^{2+} plays a role in the mitotic cycle and mating process (for review, see reference 2). A sufficient concentration of Ca^{2+} is necessary for mitotic cells to traverse the G_1 and G_2/M phases (21). Mating pheromones induce Ca^{2+} influx with a lag of approximately 30 min (22, 41, 42), followed by a rise in the cytosolic Ca^{2+} concentration ($[Ca^{2+}]_i$) (22). This rise is essential for maintaining the viability of the cells that have differentiated into cells (so-called "shmoos") having a mating projection (22). However, mutants and genes responsible for Ca^{2+} influx and Ca^{2+} signal transduction have not been isolated so far.

The mating process is triggered by the mating pheromones **a**- and α-factors, which are synthesized and secreted by *MAT***a** and *MAT*α cells, respectively (8, 17, 36, 54, 56). The mating pheromones induce orderly responses in cells of the opposite mating types. In the early stage, the pheromones induce an increase in the transcription of a small set of genes (8, 36), induce cell surface agglutinins that increase the ability to agglutinate with the other cell types (11, 33, 55), and arrest the cell division cycle at START (6, 15). In the late stage, the pheromones lead the G_1-arrested cells to differentiate into shmoos. A mating pair with shmoos of opposite mating types undergoes cell and nuclear fusion to yield a *MAT***a**/*MAT*α diploid (37, 45, 57). Finally, some of the shmoos in a mating mix that have failed to mate can recover from pheromone-induced cell cycle arrest (8).

Early events in the mating pheromone response pathway have been intensively studied because they involve mechanisms similar to those found in mammalian cells and thereby offer a model system for the genetic study of signal transduction (8, 17, 36). However, the mechanisms underlying the late events remain to be clarified, because only a limited number of genes responsible for the late events have been isolated (4, 8).

In this study, we developed a simple method for isolating yeast mutants defective in Ca^{2+} influx and possibly defective in the Ca^{2+} signaling process on the basis of our finding that *MAT***a** cells die after differentiating into shmoos when incubated with α-factor in a Ca^{2+}-deficient medium (22). We speculated that mutants that die specifically after changing into shmoos in complete medium have a defect during a late event in the mating process, and some of these mutants die because of a defect in Ca^{2+} influx or the Ca^{2+} signaling cascade. We show that the method, named the methylene blue plate (MBP) method, is effective for isolating these mutants and report that one of them, the *mid1* mutant, is indeed defective in Ca^{2+} influx and the late stage of the mating process.

MATERIALS AND METHODS

Strains, media, and pheromones. The yeast strains used in this study are listed in Table 1. Rich media and a synthetic medium, SD, were prepared as described by Sherman et al. (51). Yeast nitrogen base was prepared according to the formula given in the Difco manual (10a). Because SD medium contains 680.2 μM $CaCl_2$ and 0.8 μM calcium pantothenate, in the Ca^{2+}-deficient medium SD-Ca $CaCl_2$ was omitted and calcium pantothenate was replaced by sodium pantothenate. SD.Ca100 medium was prepared by adding 100 μM $CaCl_2$ to SD-Ca medium. Synthetic presporulation medium contained 6.7 g of yeast nitrogen base without amino acids per liter and 10 g of potassium acetate per liter. These media were supplemented with the appropriate nutrients as described in reference 51. The sporulation medium contained 10 g of potassium acetate per liter.

Escherichia coli XL1-Blue was purchased from Stratagene (La Jolla, Calif.). Competent cells were prepared with $CaCl_2$ (47) or by the method of Inoue et al. (24). Luria-Bertani medium and terrific broth were prepared as described in reference 47.

Isolation of *mid* mutants by the MBP method. Mutagenesis with ethyl methanesulfonate (Sigma, St. Louis, Mo.) was carried out essentially as described in reference 51. The parental strain, H207, contained the *sst1-2* mutation, which results in the production of a deficient protease responsible for the degradation of exported α-factor but which does not significantly affect mating and thus greatly facilitates the

* Corresponding author. Mailing address: Division of Cell Proliferation, National Institute for Basic Biology, 38 Nishigonaka, Myodaiji-cho, Okazaki 444, Japan. Phone: 81-564-55-7532. Fax: 81-564-53-7400.
† Present address: Biophysical Chemistry Laboratory, RIKEN, Saitama 351-01, Japan.

TABLE 1. *S. cerevisiae* strains used in this study

Strain	Genotype	Source or reference
Isogenic derivatives of H207		
H207[a]	*MAT***a** *his3-Δ1 leu2-3,112 trp1-289 ura3-52 sst1-2*	This work
H2071[b]	*MAT***a** *his3-Δ1 leu2-3,112 trp1-289 ura3-52*	This work
H2072[c]	*MATα his3-Δ1 leu2-3,112 trp1-289 ura3-52*	This work
H2073	*MAT***a** *leu2-3,112 trp1-289 ura3-52*	This work
H2074	*MATα his3-Δ1 trp1-289 ura3-52*	This work
H301	*MAT***a** *his3-Δ1 leu1-3,112 trp1-289 ura3-52 sst1-2 mid1-1*	This work
H3011	*MAT***a** *his3-Δ1 leu2-3,112 trp1-289 ura3-52 mid1-1*	This work
H3012	*MATα his3-Δ1 leu2-3,112 trp1-289 ura3-52 mid1-1*	This work
H3013	*MAT***a** *leu2-3,112 trp1-289 ura3-52 mid1-1*	This work
H3014	*MATα his3-Δ1 trp1-289 ura3-52 mid1-1*	This work
H207D	*MAT***a**/*MATα his3-Δ1/his3-Δ1 leu2-3,112/leu2-3,112 trp1-289/trp1-289 ura3-52/ura3-52*	This work
Isogenic derivatives of KA31		
KA31[d]	*MAT***a**/*MATα his3/his3 leu2/leu2 trp1/trp1 ura3/ura3*	25
KA31-1A	*MAT***a** *his3 leu2 trp1 ura3* (a segregant of KA31)	This work
KA31-1B	*MATα his3 leu2 trp1 ura3* (a segregant of KA31)	This work
KA31-A1	*MAT***a**/*MATα his3/his3 leu2/leu2 trp1/trp1 ura3/ura3 mid1-Δ1/MID1*	This work
KA31-B1	*MAT***a**/*MATα his3/his3 leu2/leu2 trp1/trp1 ura3/ura3 mid1-Δ2/MID1*	This work
KA31-C1	*MAT***a**/*MATα his3/his3 leu2/leu2 trp1/trp1 ura3/ura3 mid1-Δ3/MID1*	This work
KA31-D1	*MAT***a**/*MATα his3/his3 leu2/leu2 trp1/trp1 ura3/ura3 mid1-Δ4/MID1*	This work
Other strains		
X2180-1A	*MAT***a** *SUC2 mal mel gal2 CUP1*	YGSC[e]
X2180-1B	*MATα SUC2 mal mel gal2 CUP1*	YGSC
IS446-12C	*MATα met2 pha2 ade5 cyh2 his5-2$_0$ leu2-1$_0$ lys5 pet14 rna3 trp5*	YGSC
CPL1-A1-3L	*MAT***a** *MID1::LEU2 leu2-3,112*	This work

[a] This strain was constructed by crosses and dissections of the original *sst1-2* strain RC629 (7), X2180-1B, and our stock (strain HE61-6C; *MATα his3-Δ1 leu2-3,112 trp1-289 ura3-52*).
[b] The *sst1-2* allele of H207 was replaced by the *SST1* (*BAR1*) allele (35) by using the pop-in/pop-out allele replacement method (46).
[c] The mating type was switched by transformation with the plasmid YCp50-HO (18).
[d] KA31 is a *GAL*$^+$/*GAL*$^+$ strain.
[e] YGSC, Yeast Genetic Stock Center, University of California, Berkeley.

isolation of mutants defective in the α-factor response pathway (7, 35, 53). Cells mutagenized to give 60% viability were poured onto an SD-agar plate with 6 ml of SD medium containing 0.5% agar and 0.01% methylene blue and were incubated for 2 days at 30°C. This procedure was designed to result in approximately 6,000 white colonies 0.2 to 0.4 mm in diameter per plate. One milliliter of 0.1 mM α-factor was added to the plate. The plate was then rocked, uncovered, placed for about 30 min in a Clean Bench (Nihon Ikakikai, Osaka, Japan) until the surface of the agar dried, covered, and incubated for 12 to 24 h at 30°C. Colonies mainly consisting of dead cells became blue. The blue colonies were picked up with a Varipette (Eppendorf, Hamburg, Germany), suspended in 0.1 ml of SD medium, streaked onto an SD-agar plate, and incubated for 2 days at 30°C. Six colonies from each single blue colony were then suspended in 0.1 ml of SD medium containing 3 μM (5 U/ml) α-factor and 0.005% methylene blue in a 96-well plate and incubated for 10 h. Methylene blue-positive cells were identified as *mid* mutants under the microscope. Reexamination of viability in liquid medium was essential, because blue colonies were contaminated with viable cells from white colonies when α-factor was added to the plate. Cells in blue colonies are not necessarily 100% inviable, because cells in the center of the colonies are protected from the action of α-factor.

Characterization of *mid* mutants. Mutant strains (*MAT***a** *mid sst1-2*) were mated with the isogenic wild-type strain H2072 (*MATα SST1*). The resulting diploids were sporulated and the segregants (*MAT***a** *mid SST1*) were further backcrossed twice to H2072. The resulting diploids were subjected to tetrad analysis (51). After the mating type of the haploid segregants in each tetrad was determined, 10 U of α- or **a**-factor per ml was added to *MAT***a** or *MATα* segregants, respectively, that were grown in SD.Ca100. The assay mixtures were incubated for 10 h, and the viability of the segregants was examined by the methylene blue liquid method. The *mid* mutants whose mating type was α died in response to **a**-factor, although the viability of *MATα* cells is higher than that of *MAT***a** cells. The *mid* phenotype segregated $2^+:2^-$.

Genetic methods. The standard methods (51) for mating, sporulation, dissection of asci, and tetrad analysis were generally followed. Complementation between *mid* mutants and dominance versus recessiveness were tested with *MAT***a**/*MAT***a** diploids constructed by protoplast fusion between *MAT***a** strains, because *MAT***a**/*MATα* diploids do not respond to α-factor. The *mid* mutants and the parental strain with the **a** mating type were transformed by either YCp50 (*URA3*) or YEp13 (*LEU2*). Protoplasts from the resulting transformants bearing YCp50 and those bearing YEp13 were fused as described in reference 14. The fused cells were confirmed to be diploids by examining cell size and DNA content per cell, exposed to α-factor for 10 h, and mixed with 0.01% methylene blue. The viability of the fused cells was examined by counting methylene blue-positive and -negative cells under a microscope.

Recombinant DNA techniques. Extraction of plasmids, restriction endonuclease digestion, and ligation of DNA fragments were carried out as described in reference 47. Yeast chromosomal and plasmid DNAs were prepared by the method of Holm et al. (19). Oligonucleotides were synthesized

with a model 380B DNA synthesizer (Applied Biosystems, Inc., Foster City, Calif.) and were used without purification.

Cloning of the *MID1* gene by the MBP method. The *MID1* gene was isolated as follows. About 6,000 Leu^+ transformants (about 500 colonies per plate) of the *MAT***a** *mid1-1 leu2-3,112* strain (H301) were grown for 3 days at 30°C on SD-agar plates without leucine, after the introduction of a yeast genomic library carried on the YEp13 shuttle vector (59). Thereafter, 0.1 ml of 1 mM α-factor and 6 ml of SD medium containing 0.5% agar, 0.01% methylene blue, and no leucine were added, and the mixture was incubated for several additional days. Three methylene blue-negative transformants were isolated, each of which carried a plasmid responsible for complementing the *mid1-1* mutation. Restriction analysis showed that the three plasmids shared an overlapping sequence.

We proved that the cloned DNA contained the *MID1* gene by the gap-repair method (46) instead of the method of integrative mapping (see below).

Recovery of the *mid1* allele by the gap-repair method. YCpMID1-21 was digested with *Hin*dIII and religated to eliminate the 1.7-kb *Hin*dIII-*Hin*dIII fragment containing almost the entire coding region of *MID1* and its 5′-noncoding region, giving YCpMID1-21dH. YCpMID1-21dH was linearized at the *Hin*dIII site and introduced into H301 (*mid1-1*) and the parental strain, H207. The gap-repaired plasmids, designated YCpMID1-21GRM and YCpMID1-21GRW, were rescued from Leu^+ transformants of the mutant and wild-type strains, respectively. These plasmids were introduced into H301, and their ability to complement the *mid1-1* mutation was examined by the methylene blue liquid method. The results showed that YCpMID1-21GRW, but not YCpMID1-21GRM, complemented the *mid1-1* mutation. Genomic Southern blots of yeast chromosomal DNA under low-stringency conditions showed that the *MID1* gene is a single-copy gene per haploid genome. These results indicate that the complementing plasmid YCpMID101 contained the bona fide *MID1* locus.

Subcloning and DNA sequencing of the *MID1* gene. YCpMID1-1 contains the 9.8-kb *Bam*HI-*Bam*HI fragment of YEpMID101 in a low-copy vector, pRS315 (52). YEpMID1-3 and YEpMID1-4 were constructed by inserting the 5.4-kb *Bam*HI-*Pvu*II and 4.5-kb *Pvu*II-*Bam*HI fragments of YEpMID101 into the *Bam*HI and *Sma*I sites of the multicopy vector pYO325 (a derivative of pRS315 [a gift of Y. Ohya]), respectively. Deletion series plasmids YCpMID1-11 to YCpMID1-13 were constructed as follows. YEpMID1-3 was deleted from the *Bam*HI site with *Bal* 31 and cleaved at the *Xho*I site in the multicloning sites of the vector. The resulting fragments were cloned into pRS315 at the *Sma*I and *Xho*I sites. Another deletion series, YCpMID1-21 to YCpMID1-26, was constructed as follows. YEpMID1-3 was deleted from the *Apa*I region in the multicloning sites with *Bal* 31 and digested at the endogenous *Xho*I site. The resulting DNA fragments were cloned into pRS315 at the *Sma*I and *Xho*I sites. YCpMID1-23 contained the shortest complementing DNA (2.6 kb), and both strands of the insert were sequenced by dideoxy chain termination (48) with Sequenase, version 2.0 (U.S. Biochemical Corporation, Cleveland, Ohio).

Disruption of the *MID1* locus. The 3.2-kb *Bam*HI-*Sal*I fragment of YCpMID1-3 was inserted between the *Bam*HI and *Sal*I sites in pBluescript SK^+ (Stratagene), and the *Sal*I site of the resulting plasmid (EpMID1-31) was eliminated by blunt ending with mung bean nuclease and religation to give EpMID1-31S.

To construct the *mid1-Δ1* mutant (see Fig. 5B), plasmid pJJ215 bearing *HIS3* (27) was digested with *Eco*RI and *Hin*cII, which cleaves at the *Sal*I site, and the resulting *HIS3* gene cassette was inserted between the *Eco*RI and *Hin*cII sites in *MID1* on EpMID1-31S. The resulting plasmid, EpMID1-31S-EH-HIS3, in which *HIS3* is located in the opposite orientation to *MID1* to prevent the generation of the read-through transcript, was digested with *Apa*I and *Sac*II at the multicloning site. The linearized DNA was used to transform the diploid strains KA31 and H207D. To construct the *mid1-Δ2* mutant, pJJ215 was digested with *Eco*RI and *Sal*I, and the resulting *HIS3* cassette was inserted between the *Eco*RI and *Bgl*II sites in *MID1* on EpMID1-31. The resulting plasmid, EpMID1-31-EB-HIS3, was digested with *Hin*cII in *MID1* and *Spe*I at the multicloning site, and then the linearized DNA was used to transform KA31. To construct the *mid1-Δ3* and *mid1-Δ4* mutants, pJJ215 was digested with *Pst*I, and the resulting *HIS3* cassette was inserted into the *Pst*I site in *MID1* on EpMID1-31. The resulting plasmids were subjected to restriction analysis to determine the orientation of the inserted *HIS3* cassette. The plasmid having *HIS3* with the opposite orientation was named EpMID1-31-P-HIS3-1, and that having *HIS3* with the same orientation was named EpMID1-31-P-HIS3-2. These plasmids were digested with *Ssp*I in *MID1* and *Spe*I at the multicloning site to produce *mid1-Δ3* and *mid1-Δ4*. The linearized DNA was used to transform KA31. Successful disruptions of the *MID1* gene by the *HIS3* cassette were confirmed by genomic Southern blot analysis.

Genetic mapping of the *MID1* locus. The integration plasmid YIpMID-3L, which contains the *LEU2* marker gene and the *Sac*I-*Sal*I fragment carrying the entire *MID1* gene, was introduced into CPL1-A1 (*MAT***a** *leu2-3,112*). Integration of the plasmid into the chromosome was confirmed by Southern blotting. The resulting strain, CPL1-A1-3L (*MAT***a** *MID1*::*LEU2 leu2-3,112*), was subjected to standard genetic mapping (51).

Northern (RNA) blotting. Total RNA was isolated from exponentially growing cells of the haploid strains KA31-1A (*MAT***a**) and KA31-1B (*MAT*α) and the diploid strain KA31 (*MAT***a**/*MAT*α) and from KA31-1A and KA31-1B cells treated with 6 μM α-factor for 0, 15, 30, 60, 120, and 180 min by the method described by Hereford et al. (16). Purified total RNA (15 μg) was separated electrophoretically in denaturating 2.2 M formaldehyde–1% agarose gels (47) and transferred to GeneScreen nylon membrane (Du Pont-NEN). Hybridization was performed at 42°C in 50% formamide (47). The *MID1* hybridization probe was a *Hin*cII-*Hin*dIII fragment from nucleotide positions 156 to 1307 of the *MID1* DNA. The *FUS1* probe was the 0.6-kb *Ava*I-*Ava*I fragment of the plasmid pSB231 (57). The *URA3* probe was the 1.0-kb *Pst*I-*Pst*I fragment from the plasmid pJJ244 (27).

Epitope tagging. Two *FLU* sequences, each of which encodes a nine-amino-acid epitope from the influenza virus hemagglutinin (HA) antigen (58), were introduced into the multicloning site of pBluescript II SK^+ (Stratagene) by oligonucleotide-mediated site-directed mutagenesis. A sequence containing the two *FLU* sequences was fused in frame to the 3′ end of the entire *MID1* gene on YCplacMID1-23, which had been constructed with YCpMID1-23 (Fig. 5) and YCplac111 (13). The resulting plasmid, YCplacMID1-23CA5x2, contains the entire *MID1* sequence followed by the two *FLU* sequences that are separated by a 42-bp sequence corresponding to 14 amino acid residues. The first *FLU* region is preceded by a 3-bp sequence, and the second *FLU* region is followed by a 72-bp sequence (corresponding to 24 amino acid residues) and two termination codons. Therefore, a total of 57 amino acids were added just after the Mid1 protein. DNA sequencing confirmed the fusion of Mid1 and the tag. The DNA and amino acid

sequences of the fusion region containing the tag were as follows:

```
   L  D  D  T  Y  Y  P  Y  D  V  P  D  Y  A  S  R  V  D  G  I
5' - TTGGACGATACGTATTACCCTTACGACGTGCCAGATTACGCCTCTAGAGTCGACGGTATC

D  K  L  T  S  A  T  M  Y  P  Y  D  V  P  D  Y  A  S  R  I  P
GATAAGCTTACTAGTGCCACCATGTACCCTTACGACGTGCCAGATTACGCCTCTAGAATTCCT

A  A  R  G  I  L  E  R  P  P  P  R  W  S  S  S  F  C  S  L  *
GCAGCCCGGGGGATCCTAGAGCGGCCGCCACCGCGGTGGAGCTCCAGCTTTTGTTCCCTTTAG
*
TGA-3'
```

The DNA sequence of the 3'-end region of *MID1* is indicated in boldface, those of the nine-amino-acid regions are underlined, and the termination codons are indicated by asterisks. YCplacMID1-23CA5x2 completely complemented the *mid1-1* mutation, and the Mid1-2HA fusion protein was detected by Western blotting (immunoblotting) with the anti-HA monoclonal antibody 12CA5 (Berkeley Antibody Company, Richmond, Calif.).

Preparation and subcellular fractionation of cell extracts and immunoblot analysis. The methods described by Kuchler et al. (30) were generally used with slight modifications. Yeast cells were grown to mid-log phase (about 3×10^6 cells per ml) in 20 to 50 ml of SD medium supplemented with appropriate nutrients, chilled in an ice bath, harvested by centrifugation, washed once with ice-cold lysis buffer (10 mM Tris-HCl [pH 7.8], 1 mM EDTA, 2% 2-mercaptoethanol, 1 mM phenylmethylsulfonyl fluoride), and then disrupted by vortex mixing with 0.3 g of glass beads (0.45 mm in diameter) four times for 30 s each. The resulting homogenate was mixed with an appropriate volume of lysis buffer to give a final protein concentration of about 5 μg/μl. The protein concentration was determined by the method of Lowry et al. (34), and 50 μg of protein was resolved by sodium dodecyl sulfate-polyacrylamide gel electrophoresis (SDS-PAGE). If total extracts were to be directly analyzed by immunoblotting, cells were grown and harvested as described above but disrupted by vortex mixing with glass beads in 10 μl of SDS sample buffer (0.0625 M Tris-HCl [pH 6.8], 5% SDS, 10% 2-mercaptoethanol, 10% glycerol, 0.001% bromophenol blue) containing 1 mM phenylmethylsulfonyl fluoride and 50 μg of chymostatin (Sigma) per ml.

For subcellular fractionation by differential centrifugation, total cell extracts prepared as described above were sedimented at 12,000 × *g* for 30 min in a tabletop ultracentrifuge (Beckman TL100, TLA-100.3 rotor; Beckman Instruments, Inc., Fullerton, Calif.). The supernatant (S12) was separated from the resulting pellet (P12) and further sedimented at 100,000 × *g* for 1 h, producing a second pellet (P100) and supernatant fraction (S100). Each fraction was adjusted to an identical final volume, and equivalent amounts of each fraction were suspended in SDS-sample buffer containing 1 mM phenylmethylsulfonyl fluoride and 50 μg of chymostatin per ml. The suspension was incubated at 42°C for 10 min and resolved by electrophoresis in a 10 to 20% gradient gel or a 7.5% gel. The resolved proteins were electrophoretically transferred to a polyvinylidene difluoride membrane (Bio-Rad Trans-Blot transfer medium; Bio-Rad Laboratories, Hercules, Calif.) with a Bio-Rad blotting apparatus (Mini Trans-Blot cell) as recommended by the manufacturer, and Mid1, plasma membrane H^+-ATPase, and enolase were detected with the following antibodies. 12CA5, a 1:100 dilution of protein A-purified mouse monoclonal antibody against the influenza virus HA antigen was used for Mid1; a 1:25,000 dilution of ammonium sulfate concentrates of a mouse monoclonal antibody (antibody 11) was used for plasma membrane H^+-ATPase (50); and a 1:5,000 dilution of rabbit polyclonal antiserum was used for enolase (23). The immunoblots were developed with either a peroxidase-conjugated goat affinity purified antibody to mouse immunoglobulin G (Cappel, Durham, N.C. [1:2,500 dilution for Mid1 and 1:5,000 dilution for H^+-ATPase]) or a peroxidase-conjugated goat affinity-purified antibody to rabbit immunoglobulin G (Cappel [1:2,500 dilution]) and the Western blot chemiluminescence reagent Renaissance (Du Pont-NEN). The signal was detected with X-Omat AR X-ray film (Kodak, Rochester, N.Y.). To detect the Mid1-2HA fusion protein, plasma membrane H^+-ATPase, and enolase, films were usually exposed for 1 h, 5 min, and 5 to 10 s, respectively.

Nucleotide sequence accession number. The GSDB/DDBJ/EMBL/NCBI nucleotide sequence accession number for the *MID1* gene is D32133.

RESULTS

Isolation of *mid* mutants by the MBP method. We have found that *MAT***a** cells die after differentiating into shmoos when incubated with α-factor in the Ca^{2+}-deficient SD-Ca medium and are rescued when $CaCl_2$, but not $MgCl_2$, is used to supplement the medium (22). The dead shmoos consist of small cells with one projection. On the basis of this observation, we anticipated that mutants defective in the mating process because of a deficiency in Ca^{2+} influx or in the Ca^{2+} signaling process could be isolated if mutagenized cells were screened for those that died in complete SD medium only after differentiating into shmoos whose morphology was the same as that of the wild-type shmoos that died in SD-Ca medium.

We mutagenized cells of strain H207 with ethyl methanesulfonate and isolated 13 mutants that were 25% or less viable and had the morphology of small shmoos with one projection (Fig. 1) when exposed to α-factor for 10 h in SD medium, as described in Materials and Methods. We named these mutants *mid* (for mating pheromone-induced death). These mutants were classified into five complementation groups (seven *mid1*, two *mid2*, two *mid3*, one *mid4*, and one *mid5* allele), and all were recessive with single nuclear mutations. Ca^{2+} uptake of the *mid1* and *mid3* mutant strains was significantly lower than that of wild-type strains when they were incubated in the presence and absence of α-factor. Other *mid* mutants had normal Ca^{2+} uptake activity both in the presence and in the

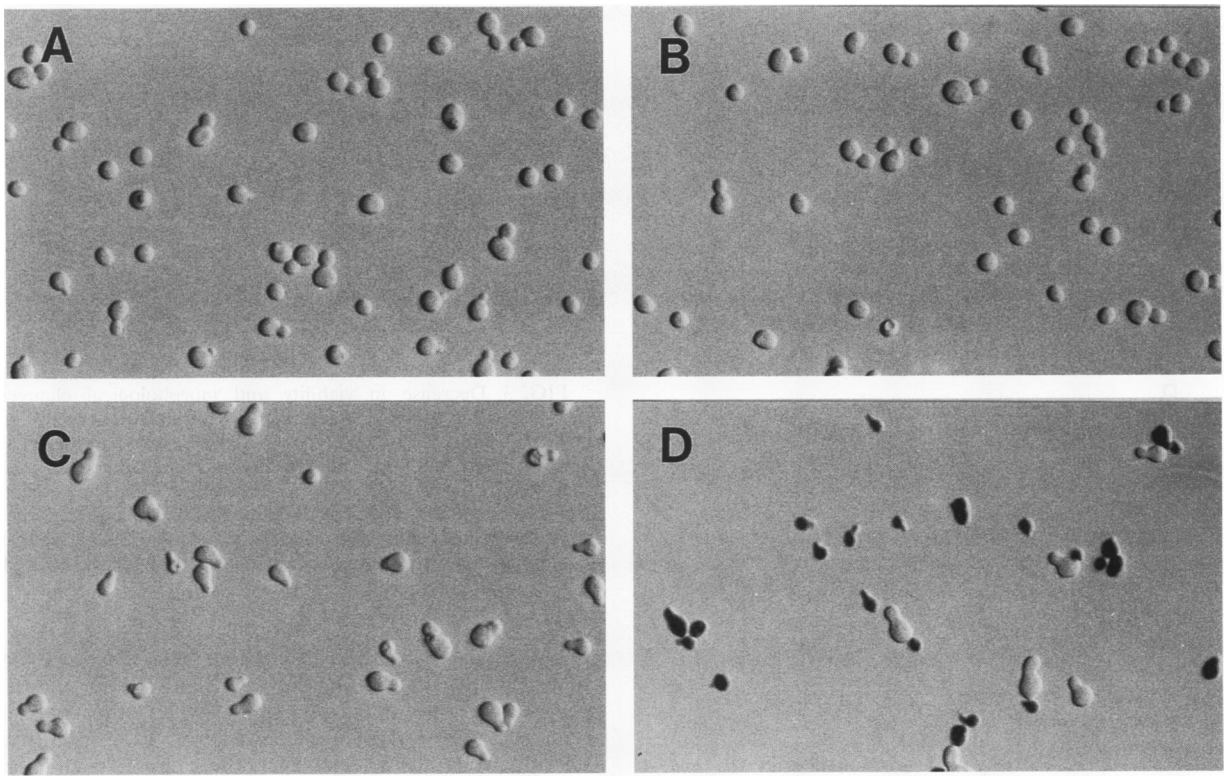

FIG. 1. Mating pheromone-induced death in the *mid1-1* mutant. (A to D) Samples were stained with methylene blue and photographed under a differential interference-contrast microscope with a ×40 objective (Nikon plan 40 DIC). Note that black cells in the photographs are methylene blue-positive and therefore inviable. (A and B) Wild-type and *mid1-1* strains H2073 and H3013, respectively, growing exponentially. (C and D) Wild-type and *mid1-1* strains H2073 and H3013, respectively, exposed to 6 μM α-factor for 3 h. In all experiments shown in this figure, cells were incubated in SD.Ca100 medium at 30°C.

absence of α-factor. The sensitivity of all of the *mid* mutants to α-factor was normal (data not shown). The *mid1-1* mutant was selected for further study.

The *mid1-1* mutant dies in response to mating pheromone because of a defect in Ca^{2+} influx. To characterize the *mid1-1* mutant, we used SD.Ca100 medium that contains 100 μM $CaCl_2$ instead of SD medium that contains 680.2 μM $CaCl_2$. The high specific radioactivity of $^{45}CaCl_2$ in SD.Ca100 medium makes it easier to evaluate the ability of Ca^{2+} uptake by the cells (especially by exponentially growing cells), and the phenotypes of the *mid* mutants are essentially the same when they are incubated in either medium.

Figure 2A shows that the Ca^{2+} uptake activity of *mid1-1* cells was lower than that of wild-type cells both in the exponentially growing phase and after exposure to α-factor for 1 h. Ca^{2+} accumulation was also lower in *mid1-1* cells than in wild-type cells when they were incubated in the presence and absence of α-factor (Fig. 2B).

We next measured the time course of mating pheromone-induced death in the *mid1-1* mutant. Cells of the *mid1-1* mutant were treated with α-factor, and the viability of the cells and percentage of shmoos were examined. Figure 3 shows that the viability was lost after a lag period of about 40 min, reaching 50% in 2.5 h and 30% in 6 h, and that differentiation into shmoos preceded the loss of viability. The latter result is consistent with the observation that all dead cells differentiated into shmoos (Fig. 1D). Similar results regarding cell viability were obtained when CFU were determined. Treatment of *MAT*α *mid1-1* cells with α-factor did not result in a loss of viability.

If the mating pheromone-induced death is due to a decrease in Ca^{2+} influx, a high concentration of Ca^{2+} in the medium should rescue the *mid1-1* cells from death. To test this possibility, $CaCl_2$, other salts (such as $MgCl_2$, $MnCl_2$, $ZnCl_2$, NaCl, and KCl), or 1 M sorbitol was added to SD-Ca medium when α-factor was added, and the viability was determined 10 h later. Figure 4 shows that α-factor-treated *mid1-1* cells were effectively rescued from death by $CaCl_2$ in a concentration-dependent manner. However, the cells were not effectively rescued by the other salts (Fig. 4) and 1 M sorbitol (data not shown). These results suggest that mating pheromone-induced death caused by the *mid1-1* mutation is due to decreased Ca^{2+} influx and indicate that the death is not due to a defect in either the incorporation of the other ions tested or the control of osmotic stability.

The *mid1* mutant is defective in mating. That the *mid1-1* mutant dies when exposed to mating pheromone suggests that mating between *MAT***a** and *MAT*α cells should be interrupted by the *mid1-1* mutation. To test this hypothesis, exponentially growing *MAT***a** and *MAT*α cells were mixed, incubated for 4 h in SD.Ca100 medium, and plated onto selection plates upon which only diploid cells can grow. Table 2 shows that diploid formation in matings between *MAT***a** *mid1-1* and *MAT*α *mid1-1* cells was reduced to approximately half that between *MAT***a** wild-type cells and *MAT*α wild-type cells. This reduction was not seen when 100 mM $CaCl_2$ was added to the medium. No reduction in matings between *MAT***a** *mid1-1* and *MAT*α wild-type cells and matings between *MAT***a** wild-type and *MAT*α *mid1-1* cells was observed. These findings indicate that the *mid1* mutation causes a bilateral mating defect.

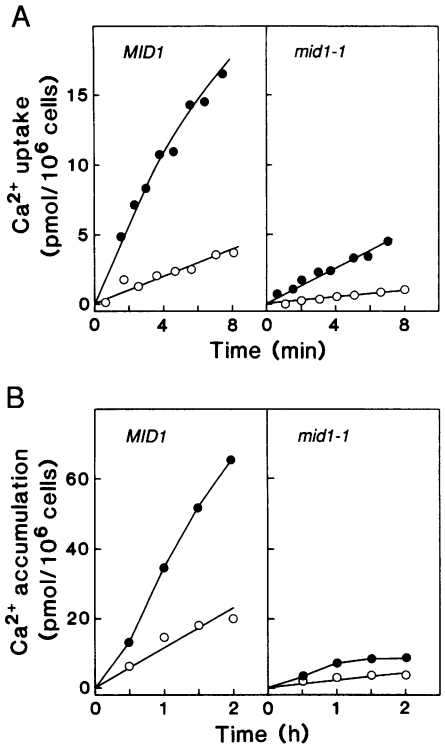

FIG. 2. Ca^{2+} uptake activity and accumulation in the *mid1-1* mutant. (A) Ca^{2+} uptake activity. Exponentially growing cells (○) and those exposed to 6 μM α-factor for 1 h (●) in SD.Ca100 medium were incubated with 185 kBq of $^{45}CaCl_2$ per ml (1.8 kBq/nmol). At the times indicated, samples were taken, filtered through Millipore filters (type HA; 0.45 μm) that had been presoaked in 5 mM $CaCl_2$ and washed five times with the same solution. The radioactivity retained on the filters was counted as described previously (22). (Left) Strain H2073 (wild type). (Right) Strain H3013 (*mid1-1*). (B) Ca^{2+} accumulation into cells in the exponentially growing phase (○) and during α-factor treatment (●) in SD.Ca100 medium. At time zero, $^{45}CaCl_2$ was added to the medium to 185 kBq/ml (1.8 kBq/nmol). For α-factor treatment, 6 μM α-factor was added to the exponentially growing culture with $^{45}CaCl_2$. Incorporation of $^{45}Ca^{2+}$ into the cells was measured as described above. (Left) Strain H2073. (Right) Strain H3013.

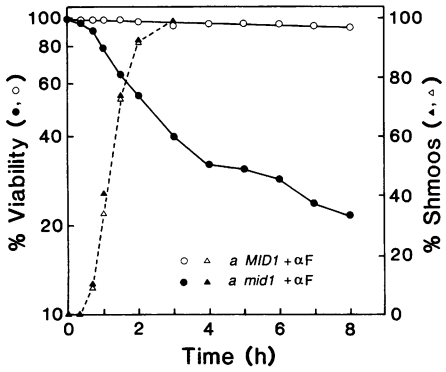

FIG. 3. Decrease in viability and morphological changes into shmoos during mating pheromone exposure. Exponentially growing cells of strains H2073 (wild type) and H3013 (*mid1-1*) received 6 μM α-factor (αF), and the cell viability was determined at the times indicated by the methylene blue liquid method (22). The percentage of shmoos was determined with the same sample. ○ and △, percentages of viability and shmoos, respectively, of H2073 cells; ● and ▲, percentages of viability and shmoos, respectively, of H3013 cells.

The sporulation efficiency of *mid1-1*/*mid1-1* diploids was essentially the same as that of wild-type diploids (data not shown).

Cloning, sequencing, and mapping of the *MID1* gene. We isolated three clones of the wild-type *MID1* gene by complementation of one of the mutant phenotypes (mating pheromone-induced death; see Materials and Methods). The three transformants were picked up, and the plasmid purified from each transformant complemented the *mid1-1* mutation. Restriction analysis showed that the three plasmids shared an overlapping sequence. One of them, YEpMID101, was further analyzed. We found that YEpMID101 complemented another mutant phenotype of *mid1-1* cells completely. The Ca^{2+} influx of the mutant bearing YEpMID101 was normal both in the exponentially growing phase and after exposure to α-factor. We demonstrated that YEpMID101 contained DNA from the bona fide *MID1* locus by the gap-repair method (see Materials and Methods).

Subcloning narrowed the location of the gene providing *MID1* complementing activity (Fig. 5A). DNA sequencing with YCpMID1-23, which contains the shortest complementing DNA, revealed a single open reading frame (ORF) encoding a polypeptide of 548 amino acids with a molecular size estimated to be 61,506 (Fig. 6). Using the BLAST homology search program (1), no significant similarity to other polypeptide sequences was found in the SwissProt, PIR, GenProt, and GPUpdate databases. However, there are four hydrophobic regions (amino acids 2 to 22, 92 to 111, 337 to 356, and 366 to 388) named H1, H2, H3, and H4, respectively (Fig. 7). The H1 segment could be a signal sequence. The sequence of the H4 segment is similar to that of the S3/H3 hydrophobic segment of a superfamily of ion channels that consists of several voltage-gated ion channels and a cyclic GMP-gated ion channel (26). There are cysteine-rich regions (amino acids 431 to 443 and 487 to 506) in the carboxy-terminal region that might be able to bind metals, although these regions did not match well with typical zinc finger motifs (3). In addition, there are 16 potential asparagine-linked (N-linked) glycosylation sites.

Pulse-field gel electrophoresis of yeast chromosome-sized DNA followed by hybridization analysis (12) with a *MID1* probe suggested that the *MID1* locus was on chromosome II or XIV. Genetic mapping showed that the *MID1* gene is located between the *MET2* locus and the *PHA2* locus on chromosome XIV (Table 3). A search of the nucleotide sequence database showed that the *MID1* gene is 0.4 kb upstream of the *RFC3* gene, which had been physically mapped to the left arm of chromosome XIV (32).

Expression of *MID1* is not transcriptionally regulated by the *MAT* locus or pheromone. Northern blot analysis of the *MID1* transcript, as well as *FUS1* and *URA3* transcripts as positive and negative controls for pheromone-dependent expression, respectively, showed that the band corresponding to the *MID1* transcript had essentially the same intensity in haploid *MAT***a** and *MAT*α cells, diploid *MAT***a**/*MAT*α cells, and *MAT***a** cells treated with α-factor for 0, 15, 30, 60, 120, and 180 min (data not shown). Only stationary cells differed. The level of the *MID1* transcript from cells incubated for 24 h in the stationary phase was about one-quarter that from exponentially growing cells. These results suggest that transcription of the *MID1* gene is not regulated by the *MAT* locus or pheromone.

Gene disruption analysis of *MID1*. Disruption of the *MID1* gene by insertion of *HIS3* cassettes was carried out by a gene replacement procedure (46). The structures of the disrupted alleles are illustrated in Fig. 5B. The results superficially

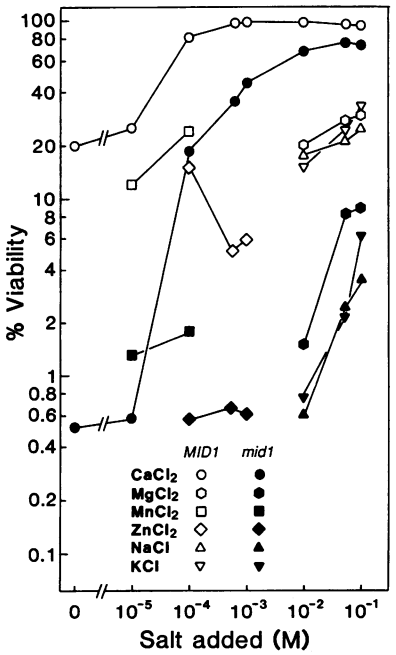

FIG. 4. Rescue from mating pheromone-induced death with Ca^{2+}. Cells growing exponentially in SD.Ca100 medium were harvested by centrifugation at 1,600 × *g*, washed twice with SD-Ca medium, resuspended in SD-Ca medium containing 6 μM α-factor and various concentrations of salts, and incubated for 10 h, after which viability was determined by the methylene blue liquid method. Strains used were H2073 (wild-type [open symbols]) and H3013 (*mid1-1* [solid symbols]). Usually SD and SD-Ca media contained 2 mM $MgSO_4$, 1.5 μM $MnSO_4$, 1.4 μM $ZnSO_4$, 1.7 mM NaCl, and 7.4 mM KH_2PO_4. During the course of these experiments, we found that $MnCl_2$ inhibited mating pheromone-induced changes into shmoos at 1 mM or higher, and thus the cells did not die. Therefore, only two concentrations of $MnCl_2$ are plotted in the figure. In the case of $ZnCl_2$, cells were killed at 10 mM or higher; therefore, viability is shown in this figure only at lower concentrations.

indicated that the *MID1* gene was essential because the disruptants, *mid1-Δ1* and *mid1-Δ2*, were inviable. However, further analysis of the disruptants indicated that the *MID1* gene is nonessential (see below).

To test whether the *MID1* gene is essential or not, the null mutant gene *mid1-Δ1* was constructed by inserting the *HIS3* cassettes into the *MID1* gene (see Materials and Methods). This construct was transformed into diploid strains (KA31 and H207D) and produced stable, viable His^+ transformants showing no growth defect. Genomic Southern blot analysis of the three independent transformants from each diploid strain showed that the disrupted copy was integrated at the *MID1* locus and had replaced the resident gene. The six His^+ transformants (*mid1-Δ1/MID1*) were then sporulated, dissected, and germinated on rich medium. In every tetrad dissected (10 to 12 tetrads for each transformant), there were two viable spores requiring histidine for growth and two nonviable spores. No His^+ spores were obtained. The same result was obtained with the *mid1-Δ2/MID1* diploid strains. By contrast, the *mid1-Δ3* and *mid1-Δ4* mutants were viable, formed normal-sized colonies, and died when exposed to α-factor, like the *mid1-1* mutant.

The results described above are consistent with two possibilities. (i) The *MID1* gene is essential, but the *mid1-Δ3* and *mid1-Δ4* alleles do not inactivate the essential function. (ii)

TABLE 2. Mating efficiency of *mid1-1* mutants

Cross[a]	Mating efficiency (%) with[b]:	
	100 μM $CaCl_2$	100 mM $CaCl_2$
*MAT***a** *MID1* × *MATα MID1*	14 ± 1	15 ± 2
*MAT***a** *MID1* × *MATα mid1-1*	14 ± 1	16 ± 2
*MAT***a** *mid1-1* × *MATα MID1*	14 ± 2	13 ± 2
*MAT***a** *mid1-1* × *MATα mid1-1*	7 ± 1	13 ± 2

[a] The isogenic strains used were H2073 (*MAT***a** *MID1*), H2074 (*MATα MID1*), H3013 (*MAT***a** *mid1-1*), and H3014 (*MATα mid1-1*).

[b] Four hours after mixing *MAT***a** and *MATα* cells in SD.Ca100 medium (which contains 100 μM $CaCl_2$) and in SD.Ca100 medium supplemented with 100 mM $CaCl_2$, mating efficiency was determined as described previously (22).

The *MID1* gene is not essential, and the *mid1-Δ1* and *mid1-Δ2* alleles interfere with expression of an adjacent, essential gene. The following experiments support this latter possibility. The *mid1-Δ1* and *mid1-Δ2* mutations were not complemented by the plasmids YCpMID1-21, YCpMID1-22, and YCpMID1-23, which complement the original *mid1-1* mutation (Table 4). The diploid strains *mid1-Δ1/MID1* and *mid1-Δ2/MID1* were transformed by each of these plasmids, sporulated, and dissected. In every tetrad dissected (30 to 40 tetrads for each transformant), there were two viable His^- spores and two nonviable spores.

By the same experimental procedures, we obtained the surprising result that the *mid1-Δ1* mutation was complemented by YCpMID1-11, YCpMID1-12, and YCpMID1-13, which do not contain the complete *MID1* gene and thereby do not complement the original *mid1-1* mutation (Table 4). The same results were obtained with the *mid1-Δ2* mutation. YCpMID1-11 and YCpMID1-12 contain the entire ORF of the essential gene *RFC3* and its 5′-flanking region as well as the 5′ portion of the *MID1* ORF. YCpMID1-13 contains the entire ORF of the *RFC3* gene with a limited portion (27 bp long) of its 5′-flanking region.

Haploid strains *mid1-Δ1*/YCpMID1-11, *mid1-Δ1*/YCpMID1-12, and *mid1-Δ1*/YCpMID1-13 showed essentially the same phenotype regarding α-factor-induced death as the original *mid1-1* mutant. In addition, 10 mM $CaCl_2$ rescued these mutant cells from α-factor-induced death. This result strongly suggests that the cloned and disrupted gene is *MID1*, not the *RFC3* gene. The gap-repair method has also shown that the cloned gene is *MID1* as described above. We therefore conclude that the *MID1* gene is not essential for growth and suggest that some deletions of the ORF of the *MID1* gene impair the expression of the adjacent gene, *RFC3*. There may be a sequence or a structure important for the expression of the *RFC3* gene in the ORF of the *MID1* gene.

The *MID1* gene product (Mid1) is a plasma membrane protein. The predicted amino acid sequence of the *MID1* gene product (Mid1) contains four hydrophobic regions, one of which (H4) is partially homologous to the S3/H3 membrane-spanning domain of several ion channels (Fig. 7). We therefore anticipated that Mid1 is a membrane protein and that its intracellular localization could be unambiguously determined. The intracellular location was determined by subcellular fractionation and various extraction procedures followed by immunoblotting with a functional epitope-tagged Mid1 protein, in which two nine-amino-acid epitopes from the influenza HA with flanking regions were fused to the carboxy-terminal amino acid of Mid1 (see Materials and Methods). Neither potential membrane-spanning domains nor N-glycosylation sites were present in the tag. Strain H3013 (*MAT***a** *mid1-1 leu2-3,112*) was transformed with a centromere-based plasmid containing the

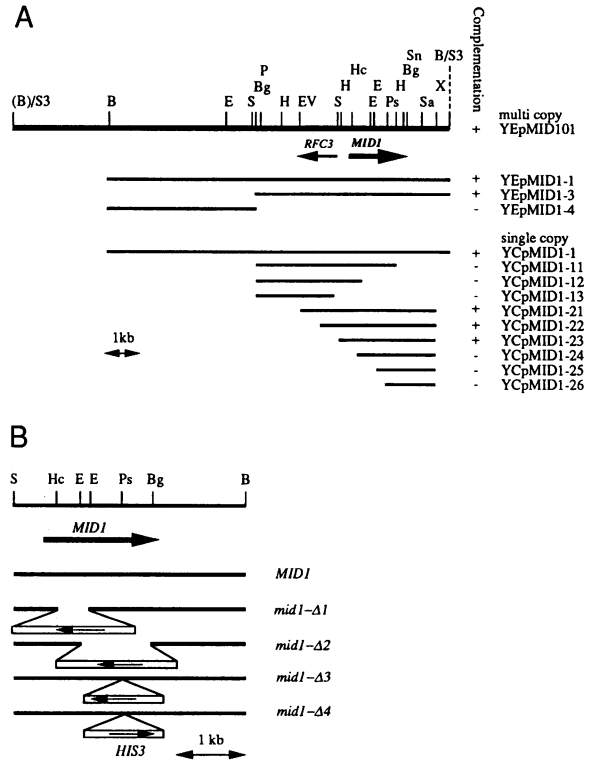

FIG. 5. Analysis of the *MID1* gene. (A) Restriction map and subcloning of the *MID1* gene. The large arrow indicates the location and direction of the *MID1* ORF. The small arrow indicates the location and direction of the *RFC3* ORF. The initiation codon of the *RFC3* gene overlaps a *Sal*I site. Subclones are indicated by bars, and the ability of the subclones to complement the α-factor-induced death phenotype associated with the *mid1-1* mutation is indicated by + or −. YCpMID1-23 was used for sequencing DNA. Restriction endonucleases are abbreviated as follows: B, *Bam*HI; Bg, *Bgl*II, E, *Eco*RI; EV, *Eco*RV; H, *Hin*dIII; Hc, *Hin*cII; P, *Pvu*II; Ps, *Pst*I; S, *Sal*I; S3, *Sau*3A; Sa, *Sac*I; Sn, *Sna*BI; X, *Xho*I. (B) Disruption of the *MID1* gene. Solid bars indicate the *MID1* locus and open boxes indicate the *HIS3* cassettes. Large and small arrows indicate the locations and directions of the *MID1* and *HIS3* ORFs, respectively. The abbreviations for restriction endonucleases are the same as those described for panel A.

epitope-tagged Mid1 construct (YCplacMID1-23CA5x2). The Leu^+ transformants containing this plasmid grew normally, no longer died when exposed to α-factor, and were normal in Ca^{2+} influx, indicating that the epitope-tagged Mid1 protein is not toxic and fully complements the *mid1-1* mutation. Control cells transformed with untagged *MID1* (YCplacMID1-23) were prepared in parallel for some experiments.

Anti-HA monoclonal antibody 12CA5 recognized a 100-kDa protein specific to cells having the plasmid YCplacMID1-23CA5x2 (Fig. 8A, lanes 1 and 2). The observed molecular mass of the epitope-tagged Mid1 differs from that predicted by the nucleotide sequence of the fusion gene (68 kDa). The presence of 16 potential N-linked glycosylation sites in the Mid1 sequence may account for this difference in size. We tested this notion with tunicamycin, an inhibitor of N-linked glycosylation. A single culture was divided into two equal parts. One was incubated for 2.5 h with tunicamycin, and the other received dimethyl sulfoxide, a solvent for tunicamycin. Figure 8B shows that the 100-kDa protein was not present but that a 68-kDa protein appeared in tunicamycin-treated cells, indicating that Mid1 is N glycosylated.

To determine whether Mid1 is a membrane protein, the partitioning of the epitope-tagged Mid1 protein by differential centrifugation was compared with that of known marker proteins. Figure 8A shows that, like the plasma membrane H^+-ATPase, the bulk of the total cellular content of the epitope-tagged Mid1 protein sedimented at 12,000 × *g*. In contrast, the majority of a soluble protein, enolase, remained in the supernatant fraction after sedimentation at both 12,000 × *g* and 100,000 × *g*. These results suggest that Mid1 is a membrane protein.

To determine whether Mid1 is indeed an integral membrane protein, total cell extracts were incubated with various solubilizing agents and sedimented at 100,000 × *g*, and equivalent portions of the resulting pellet and supernatant fractions were analyzed by immunoblotting. Figure 8C shows that the majority of the epitope-tagged Mid1 protein was not released into the supernatant by treatment with high levels of salt, sodium carbonate (pH 11), or urea, all of which extract peripheral membrane proteins. The nonionic detergent Triton X-100 and the strong anionic detergent SDS efficiently solubilized the epitope-tagged Mid1 protein from membranes. The plasma membrane H^+-ATPase, but not enolase, behaved similarly under the same conditions. These results suggest that Mid1 is an integral membrane protein.

To determine whether Mid1 is a plasma membrane protein, intact cells were incubated with Zymolyase, which contains proteases and endoglucanases (49). Figure 8D shows that all of the epitope-tagged Mid1 protein with a native molecular weight of 100 kDa disappeared and an 80-kDa protein appeared in the Zymolyase-treated cells. No other polypeptide with a smaller molecular size specific to cells expressing the epitope-tagged Mid1 was observed. The 80-kDa protein disappeared when the cells were incubated with Zymolyase in the presence of Triton X-100. These results suggest that Mid1 is located in the plasma membrane and that at least a portion of the Mid1 polypeptide is exposed to the exocellular surface. The appearance of the 80-kDa protein seems to be consistent with the idea that the carboxy-terminal portion of the Mid1 polypeptide is exposed to the cytoplasm because the epitope has been fused to the carboxy-terminal amino acid of this polypeptide. However, further experiments are needed to determine the exact membrane orientation of Mid1.

On the basis of these observations, we conclude that Mid1 is an integral plasma membrane protein with N-linked carbohydrate.

DISCUSSION

Detecting a new conditional phenotype. This report introduces a new conditional phenotype regarding pheromone response and Ca^{2+} signaling. We isolated conditional mutants of *S. cerevisiae*, designated *mid* mutants, that die specifically after receiving the mating pheromone, α-factor. These mutants were classified into five complementation groups. The idea of isolating *mid* mutants was based on our recent finding that wild-type yeast cells die in response to α-factor after differentiating into shmoos when Ca^{2+} influx stimulated by the pheromone is inhibited by incubating the cells in Ca^{2+}-deficient medium (22). We thus anticipated that screening for mutants that die specifically after differentiating into shmoos in a medium containing a sufficient concentration of Ca^{2+} should allow the isolation of mutants defective in Ca^{2+} influx or Ca^{2+} signal transduction during the mating process. The *mid1* and *mid3* mutants are indeed defective in Ca^{2+} influx, and other *mid* mutants, *mid2*, *mid4*, and *mid5*, are normal with regard to Ca^{2+} influx. As expected, the terminal phenotypes regarding

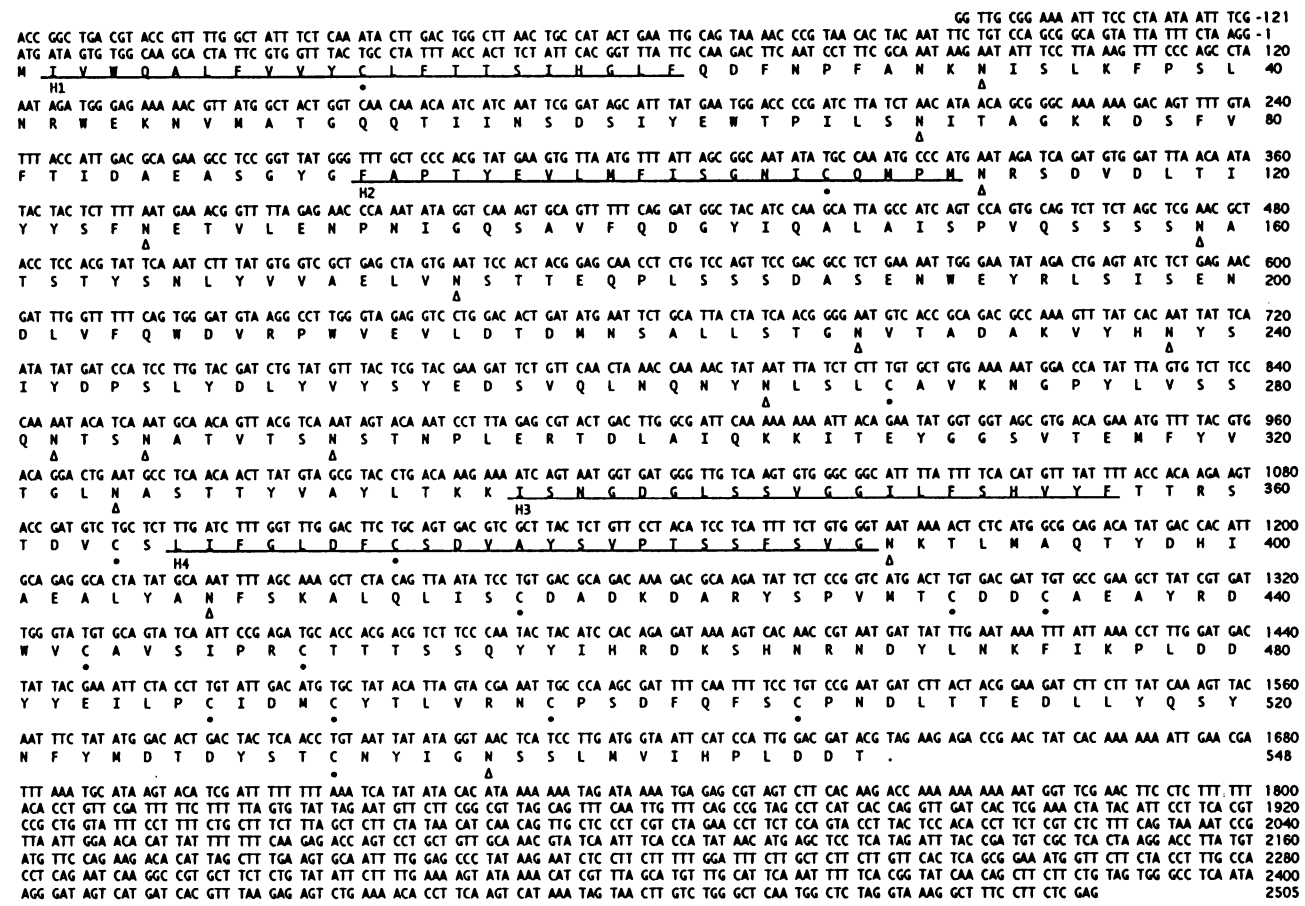

FIG. 6. DNA sequence and corresponding deduced amino acid sequence of the *MID1* gene. The *MID1* ORF consists of 1,644 nucleotides and is 548 amino acids long. The numerals in the right margin indicate nucleotide and amino acid positions. Nucleotide 1 corresponds to the first nucleotide of the initiation codon, and amino acid 1 corresponds to the first residue of the deduced protein. Four hydrophobic segments (H1, H2, H3, and H4) are underlined. Cysteine residues are marked by closed circles. Potential N-linked glycosylation sites are marked by open triangles.

the morphology and viability of these mutants are essentially the same as those of wild-type cells exposed to α-factor in a Ca^{2+}-deficient medium (22) (Fig. 1 and 3).

Many mutants defective in early events during the mating process are isolated because such mutations result in resistance to the growth-inhibitory effect of α-factor. Molecular analysis of these mutants has identified genes encoding pheromone receptors, heterotrimeric G proteins, protein kinases, and a transcription activator (8, 36, 54). In contrast to these mutants, all of the *mid* mutants differentiate normally into shmoos in response to α-factor and then die. This observation indicates that the early events in the mating process are not affected by the *mid* mutations. Although several mutants defective in late events such as cell and nuclear fusion have been isolated and characterized (4, 5, 37, 38, 44, 45, 57), neither conditional lethality caused by the action of mating pheromones nor deficiency of Ca^{2+} regulation has been reported.

Roles of the *MID1* gene. The predicted *MID1* gene product (Mid1) is 548 amino acids long and has a molecular mass estimated to be 61,506 Da. No extensive homology to any known proteins has been identified. However, there are two structural features of interest in the predicted amino acid sequence.

The first is the presence of four hydrophobic segments, one of which (H4 [Fig. 6 and 7]) is homologous to the membrane-spanning region (S3/H3) present in several ion channels, including voltage-gated Ca^{2+} channels (26). Immunodetection of Mid1 indicated that it is N glycosylated and spans the plasma membrane (Fig. 8). We thus propose that Mid1 is an integral plasma membrane protein required for Ca^{2+} influx. However, we do not yet know whether Mid1 is a component of a Ca^{2+} channel or transporter. Even if Mid1 functions as an ion channel or transporter, it appears not to function alone, because overexpression of the *MID1* gene on a multicopy vector does not affect Ca^{2+} influx (data not shown).

The second feature is the presence of two carboxy-terminal cysteine-rich regions. In general, such regions often constitute zinc finger motifs that function in DNA binding or protein-protein interactions (3, 43). Considering the location and modification of Mid1, we suppose that if the carboxy-terminal cysteine-rich regions have a function, they might play a role in protein-protein interactions on the plasma membrane leading to Ca^{2+} influx rather than to DNA binding.

The *mid1-1* mutant displays unique phenotypes during the mating process, and these phenotypes appear to be due to a deficiency of Ca^{2+} influx as follows. (i) Stimulation of Ca^{2+} influx in *mid1-1* cells by α-factor is low (Fig. 2). (ii) After receiving α-factor, *mid1-1* cells die with a lag of about 40 min (Fig. 3). (iii) *mid1-1* cells can survive in the presence of mating pheromone if sufficient Ca^{2+}, but not Mg^{2+}, Mn^{2+}, Zn^{2+},

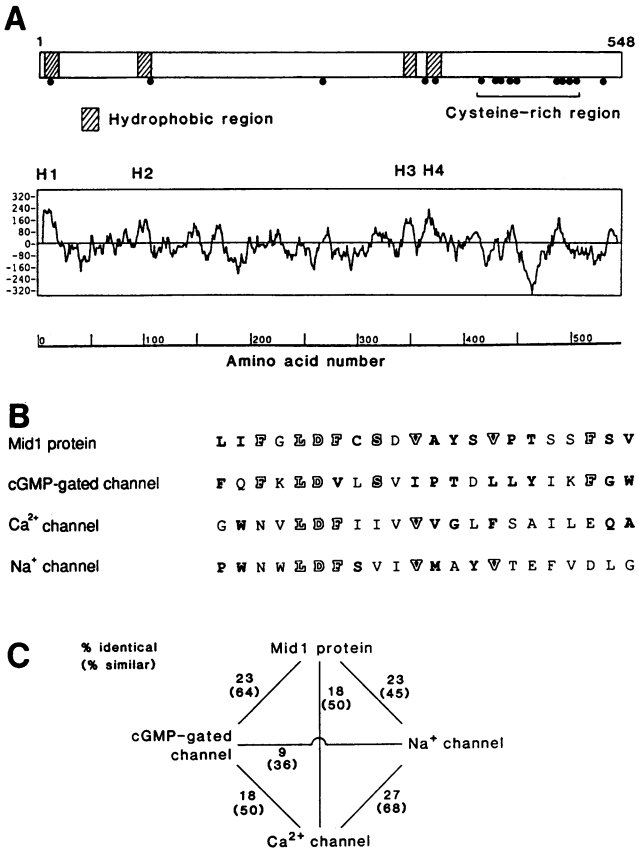

FIG. 7. Characteristics of the Mid1 protein. (A) Schematic diagram and hydropathy profile of the Mid1 protein. (Top) The hydrophobic regions, H1, H2, H3, and H4, are indicated by hatched boxes. Cysteine residues are indicated by solid circles. (Middle) Hydropathy profile predicted by the Kyte and Doolittle hydropathy algorithm (31). The default is 11 (5 before and 5 after a given residue). (Bottom) Position numbers of amino acid residues. (B) Multiple sequence alignment of the H4 segment of the Mid1 protein and the S3/H3 segments of ion channels. Identical and chemically similar residues between the Mid1 protein and ion channels are described in outline and boldface types, respectively. Typical examples of similarity are presented here. For more examples, see the article by Jan and Jan (26). The sequences for the H3 domain of the bovine rod photoreceptor cyclic GMP (cGMP) gated ion channel (28), the S3 domain of the rabbit cardiac dihydropyridine-sensitive calcium channel (39), and the S3 domain of the rat brain sodium channel type III (29) are shown. (C) Schematic representation of sequence similarities between the Mid1 protein and ion channels shown above. The numerals indicate the percentage of identical amino acids between the two proteins and those in parentheses indicate the percentage of identical and chemically similar amino acids between the two proteins. The chemically similar amino acids are as follows: nonpolar, A, F, I, L, M, P, V, and W; uncharged polar, C, G, Q, S, T, and Y.

Na^+, K^+, or sorbitol, is added to the medium (Fig. 4). (iv) Matings between *MAT***a** *mid1-1* and *MAT*α *mid1-1* cells are restricted, except in media containing a high concentration of Ca^{2+} (Table 2). These phenotypes are essentially the same as those observed in wild-type cells treated with α-factor in a Ca^{2+}-deficient medium (22). Thus we conclude that the *MID1* gene product is required for Ca^{2+} influx.

The possible targets of Ca^{2+} mobilized by the *MID1* gene product could be Ca^{2+}-binding proteins. In terms of mating regulation, the yeast homolog of calcineurin, a Ca^{2+}/calmodulin-dependent phosphoprotein phosphatase, is of interest. It consists of the catalytic subunit (A) that binds calmodulin and the regulatory subunit (B) that binds Ca^{2+}. Binding of both Ca^{2+} and calmodulin to the A-B complex yields its full activity. The double-null mutant of the A subunit, in which both of the related genes *CNA1* (*CMP1*) and *CNA2* (*CMP2*) are disrupted, is defective in the ability to recover from α-factor-induced growth arrest (9). Similar results have been obtained with the null mutant of the B subunit gene *CNB1* (10). Interestingly, the Δ*cmp1* Δ*cmp2* and Δ*cnb1* cells (40) died after differentiating into shmoos, although the viability of these cells was slightly higher than that of the *mid1* mutant (20). Therefore, Mid1 and the calcineurin homolog may function in a Ca^{2+} signal transduction pathway.

TABLE 3. Genetic mapping of the *MID1* gene[a]

Gene pair	No. of asci with the following tetrad type[b]:			Map distance (cM)[c]
	PD	NPD	T	
MID1::*LEU2-met2*	33	0	14	14.9
MID1::*LEU2-pha2*	22	0	25	26.6
met2-pha2	19	0	28	29.8

[a] Strain CPL1-A1-3L (*MAT***a** *MID1*::*LEU2 leu2*) was crossed with strain IS446-12C (*MAT*α *met2 pha2 leu2*). The resulting diploid was subjected to meiosis and spore formation. Ninety percent of the tetrads produced four viable spores.
[b] Abbreviations: PD, parental ditype; NPD, nonparental ditype; T, tetratype.
[c] cM, centimorgans.

Effect of disruption of the *MID1* gene. Gene disruption analysis is based on the assumption that disruption of a gene of interest does not affect the expression of adjacent genes. As far as we know, there has been no exception to this assumption in eukaryotic chromosomes. The present study suggested that disruption of the *MID1* gene impairs the expression of an essential gene, *RFC3*, which is located 0.4 kb upstream of the *MID1* gene in the opposite orientation. The ORF of the *MID1* gene could contain some important sequence for the transcription of the *RFC3* gene. Further molecular analyses should clarify the regulation mechanism of the expression of the *RFC3* gene.

TABLE 4. Tetrad distribution showing suppression of the *mid1-Δ1* mutation by several plasmids[a]

Plasmid	Tetrad distribution				
	$4^+:0^-$[b]	$3^+:1^-$	$2^+:2^-$	$1^+:3^-$	$0^+:4^-$
YCpMID1-1	2	9	2	1	0
YCpMID1-11	4	5	4	1	0
YCpMID1-12	1	3	7	1	0
YCpMID1-13	5	3	3	0	0
YCpMID1-21	0	0	13	1	0
YCpMID1-22	0	0	14	0	0
YCpMID1-23	0	0	14	0	0
pRS315	0	0	14	0	0

[a] Strain KA31-A1 (*MAT***a**/*MAT*α *mid1-Δ1*::*HIS3*/*MID1*) containing each of the plasmids (whose selection marker was *LEU2*) listed in this table was sporulated. Tetrads were dissected and germinated. Two His^- Leu^+ spores were obtained in each tetrad that segregated $4^+:0^-$. One His^- Leu^+ spore was obtained in each tetrad that segregated $3^+:1^-$. No His^+ spore was obtained in each tetrad that segregated $2^+:2^-$ and $1^+:3^-$.
[b] +, viable spore; −, inviable spore.

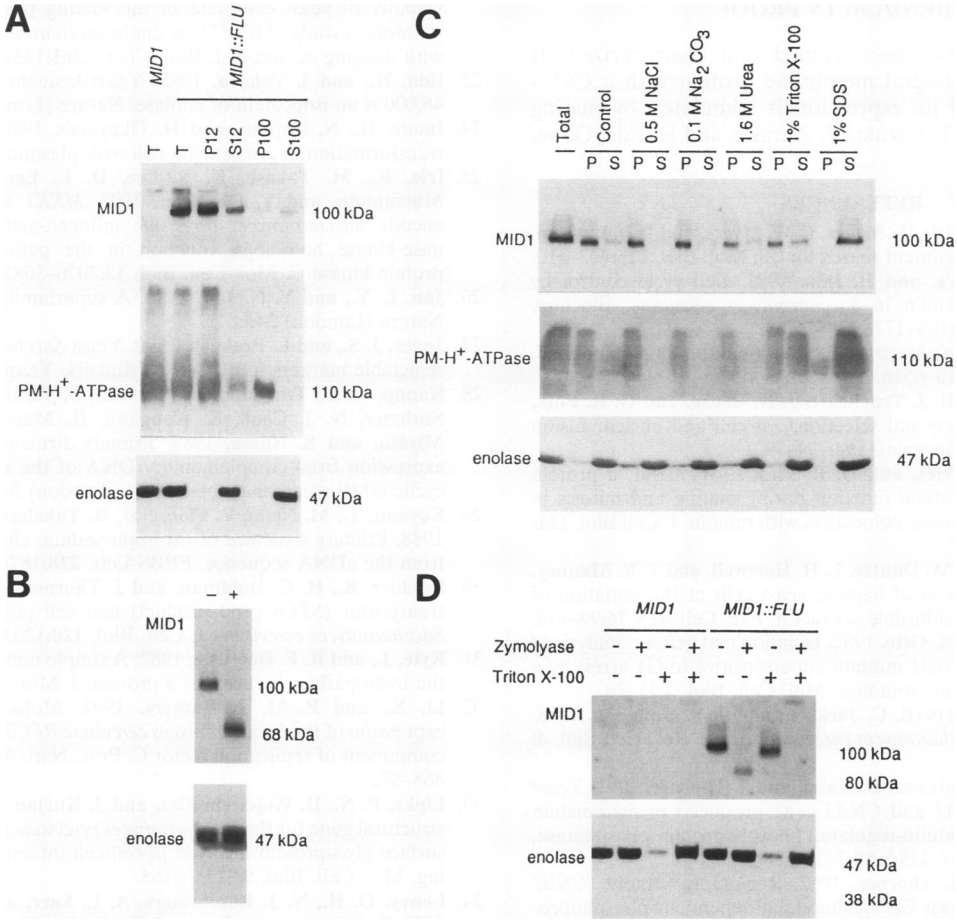

FIG. 8. Detection of Mid1 protein by immunoblotting. (A) Mid1 protein cofractionates with an authentic plasma membrane marker protein. Total cell extracts prepared from H3013 cells bearing YCplacMID1-23 or YCplacMID1-23CA5x2 were fractionated by differential centrifugation, and the content of Mid1, plasma membrane H^+-ATPase (PM-H^+-ATPase), and enolase was determined by SDS-PAGE (10 to 20% polyacrylamide for Mid1 and enolase; 7.5% polyacrylamide for plasma membrane H^+-ATPase) and immunoblotting as described in Materials and Methods. *MID1*, a sample prepared from H3013 cells bearing YCplacMID1-23; *MID1::FLU*, a sample prepared from H3013 cells bearing YCpMID1-23CA5x2; T, total extract; P12 and S12, pellet and supernatant fraction, respectively, of a 12,000 × *g* sedimentation of total extract; P100 and S100, pellet and supernatant fraction, respectively, of a 100,000 × *g* sedimentation of S12. The plasma membrane H^+-ATPase was smeared because of low solubility. (B) Mid1 protein is N glycosylated. A culture of H3013 cells bearing YCplacMID1-23CA5x2 was split into two aliquots, one of which received 10 μg of tunicamycin per ml; the other received dimethyl sulfoxide, the solvent of a stock solution of this drug. These cultures were incubated for 2.5 h, and the cells were then subjected to SDS-PAGE (10% polyacrylamide) and immunoblotting. + and −, treated and not treated with tunicamycin, respectively. (C) Mid1 protein is an integral membrane protein. The solubilizing agents indicated in the figure were added to aliquots of the supernatant of a low-speed centrifugation (at 600 × *g*) of the total cell extracts prepared from H3013 cells bearing YCplacMID1-23CA5x2. After incubation at 4°C for 20 min, samples were centrifuged at 100,000 × *g* for 1 h to separate the pellet (P) and supernatant (S) fractions, followed by SDS-PAGE (10% polyacrylamide) and immunoblotting. A small amount of an isoprotein of enolase (48 kDa; hsp48) was detected on this immunoblot (23). (D) Mid1 protein is accessible to proteolysis in intact cells. H3013 cells bearing YCplacMID1-23 (control) or YCplacMID1-23CA5x2 were harvested, resuspended in spheroplasting buffer (1.2 M sorbitol, 60 mM EDTA, 100 mM citrate [pH 6.8]), and incubated with 100 μg of Zymolyase-100T per ml for 30 min at 30°C in the presence or absence of 1% Triton X-100. Thereafter, all samples, except for that treated with Zymolyase in the presence of Triton X-100, were washed once with spheroplasting buffer. The samples were then homogenized with glass beads in SDS-sample buffer containing 1 mM phenylmethylsulfonyl fluoride and 50 μg of chymostatin per ml and analyzed by SDS-PAGE (10 to 20% polyacrylamide) and immunoblotting. Enolase appeared to leak from the cells during exposure to Triton X-100 and washing with spheroplasting buffer. Proteases in Zymolyase preparations digest enolase poorly and produce a limited amount of a 38-kDa polypeptide.

ACKNOWLEDGMENTS

We thank Satoshi Harashima for advice on protoplast fusion; Gerald R. Fink, Philip Hieter, Masahiro Ishiura, Vivian L. MacKay, Kunihiro Matsumoto, Kenji Moriyama, Satoshi Nomoto, Yoshikazu Ohya, Akio Sugino, and Kazuma Tanaka for supplying plasmids; Yoshiko Kikuchi, Kunihiro Matsumoto, and Tokichi Miyakawa for yeast strains; Mark Goebl, Fumio Hanaoka, Masato Ishikawa, Tomoki Miwa, Kenta Nakai, and Toshiki Ohkawa for help with the homology search; Ramon Serrano for supplying antibody; Yoshiyuki Imai for sequencing DNA of the junction region of epitope-tagged Mid1; Katsunori Aizawa and Yoshihiko Fujita for an immunoblot apparatus; and Goro Eguchi, Ikuo Takeuchi, and Masayuki Yamamoto for encouragement.

This work was supported in part by Grants-in-Aid for Scientific Research on Priority Areas 04256104 and 04266225 to H.I. and Grants-in-Aid for Scientific Research 04833028 to H.I. and 63440088 and 03557102 to Y.A. from the Ministry of Education, Science and Culture of Japan and by The Naito Foundation (H.I).

ADDENDUM IN PROOF

The *MID2* gene has been cloned and characterized. It encodes a putative integral membrane protein with a Ca^{2+}-binding domain, and its expression is stimulated by mating pheromone (T. Ono, T. Suzuki, Y. Anraku, and H. Iida, Gene, in press).

REFERENCES

1. **Altschul, S. F., W. Gish, W. Miller, E. W. Myers, and D. J. Lipman.** 1990. Basic local alignment search tool. J. Mol. Biol. **215**:403–410.
2. **Anraku, Y., Y. Ohya, and H. Iida.** 1991. Cell cycle control by calcium and calmodulin in *Saccharomyces cerevisiae*. Biochim. Biophys. Acta **1093**:169–177.
3. **Berg, J. M.** 1990. Zinc fingers and other metal-binding domains. J. Biol. Chem. **265**:6513–6516.
4. **Berlin, V., J. A. Brill, J. Trueheart, J. D. Boeke, and G. R. Fink.** 1991. Genetic screens and selections for cell and nuclear fusion mutants. Methods Enzymol. **194**:774–792.
5. **Berlin, V., C. A. Styles, and G. R. Fink.** 1990. BIK1, a protein required for microtubule function during mating and mitosis in *Saccharomyces cerevisiae*, colocalizes with tubulin. J. Cell Biol. **111**: 2573–2586.
6. **Bücking-Throm, E., W. Duntze, L. H. Hartwell, and T. R. Manney.** 1973. Reversible arrest of haploid yeast cells at the initiation of DNA synthesis by a diffusible sex factor. Exp. Cell Res. **76**:99–110.
7. **Chan, R. K., and C. A. Otte.** 1982. Isolation and genetic analysis of *Saccharomyces cerevisiae* mutants supersensitive to G1 arrest by a factor and α factor pheromones. Mol. Cell. Biol. **2**:11–20.
8. **Cross, F., L. H. Hartwell, C. Jackson, and J. B. Konopka.** 1988. Conjugation in *Saccharomyces cerevisiae*. Annu. Rev. Cell Biol. **4**: 429–457.
9. **Cyert, M. S., R. Kunisawa, D. Kaim, and J. Thorner.** 1991. Yeast has homologs (*CNA1* and *CNA2* gene products) of mammalian calcineurin, a calmodulin-regulated phosphoprotein phosphatase. Proc. Natl. Acad. Sci. USA **88**:7376–7380.
10. **Cyert, M. S., and J. Thorner.** 1992. Regulatory subunit (*CNB1* gene product) of yeast Ca^{2+}/calmodulin-dependent phosphoprotein phosphatases is required for adaptation to pheromone. Mol. Cell. Biol. **12**:3460–3469.

10a. **Difco Laboratories.** 1984. Difco manual, 10th ed., p. 1135–1141. Difco Laboratories, Detroit.

11. **Fehrenbacher, G., K. Perry, and J. Thorner.** 1978. Cell-cell recognition in *Saccharomyces cerevisiae*: regulation of mating-specific adhesion. J. Bacteriol. **134**:893–901.
12. **Gerring, S. L., C. Connelly, and P. Hieter.** 1991. Positional mapping of genes by chromosome blotting and chromosome fragmentation. Methods Enzymol. **194**:57–77.
13. **Gietz, R. D., and A. Sugino.** 1988. New yeast-*Escherichia coli* shuttle vectors constructed with in vitro mutagenized yeast genes lacking six-base-pair restriction sites. Gene **74**:527–534.
14. **Harashima, S., A. Takagi, and Y. Ohshima.** 1984. Transformation of protoplasted yeast cells is directly associated with cell fusion. Mol. Cell. Biol. **4**:771–778.
15. **Hartwell, L. H.** 1973. Synchronization of haploid yeast cell cycles, a prelude to conjugation. Exp. Cell Res. **76**:111–117.
16. **Hereford, L. M., M. A. Osley, J. R. Ludwig II, and C. S. McLaughlin.** 1981. Cell-cycle regulation of yeast histone genes H2A and H2B. Cell **18**:1261–1271.
17. **Herskowitz, I.** 1988. Life cycle of the budding yeast *Saccharomyces cerevisiae*. Microbiol. Rev. **52**:536–553.
18. **Herskowitz, I., and R. E. Jensen.** 1991. Putting the *HO* gene to work: practical uses for mating-type switching. Methods Enzymol. **194**:132–146.
19. **Holm, C., D. W. Meeks-Wagner, W. L. Fangman, and D. Botstein.** 1986. A rapid, efficient method for isolating DNA from yeast. Gene **42**:169–173.
20. **Iida, H.** Unpublished data.
21. **Iida, H., S. Sakaguchi, Y. Yagawa, and Y. Anraku.** 1990. Cell cycle control by Ca^{2+} in *Saccharomyces cerevisiae*. J. Biol. Chem. **265**: 21216–21222.
22. **Iida, H., Y. Yagawa, and Y. Anraku.** 1990. Essential role for induced Ca^{2+} influx followed by $[Ca^{2+}]_i$ rise in maintaining viability of yeast cells late in the mating pheromone response pathway: a study of $[Ca^{2+}]_i$ in single *Saccharomyces cerevisiae* cells with imaging of fura-2. J. Biol. Chem. **265**:13391–13399.
23. **Iida, H., and I. Yahara.** 1985. Yeast heat-shock protein of Mr 48,000 is an isoprotein of enolase. Nature (London) **315**:688–690.
24. **Inoue, H., N. Nojima, and H. Okayama.** 1990. High frequency transformation of *Escherichia coli* with plasmids. Gene **96**:23–28.
25. **Irie, K., M. Takase, K. S. Lee, D. E. Levin, H. Araki, K. Matsumoto, and Y. Ohshima.** 1993. *MKK1* and *MKK2*, which encode *Saccharomyces cerevisiae* mitogen-activated protein kinase-kinase homologs, function in the pathway mediated by protein kinase C. Mol. Cell. Biol. **13**:3076–3083.
26. **Jan, L. Y., and Y. N. Jan.** 1990. A superfamily of ion channels. Nature (London) **345**:672.
27. **Jones, J. S., and L. Prakash.** 1990. Yeast *Saccharomyces cerevisiae* selectable markers in pUC18 polylinkers. Yeast **6**:363–366.
28. **Kaupp, U. B., T. Niidome, T. Tanabe, S. Terada, W. Bonigk, W. Stuhmer, N. J. Cook, K. Kangawa, H. Matsuo, T. Hirose, T. Miyata, and S. Numa.** 1989. Primary structure and functional expression from complementary DNA of the rod photoreceptor cyclic GMP-gated channel. Nature (London) **342**:762–766.
29. **Kayano, T., M. Noda, V. Flockerzi, H. Takahashi, and S. Numa.** 1988. Primary structure of rat brain sodium channel III deduced from the cDNA sequence. FEBS Lett. **228**:187–194.
30. **Kuchler, K., H. G. Dohlman, and J. Thorner.** 1993. The a-factor transporter (*STE6* gene product) and cell polarity in the yeast *Saccharomyces cerevisiae*. J. Cell. Biol. **120**:1203–1215.
31. **Kyte, J., and R. F. Doolittle.** 1982. A simple method for displaying the hydropathic character of a protein. J. Mol. Biol. **157**:105–132.
32. **Li, X., and P. M. J. Burgers.** 1994. Molecular cloning and expression of the *Saccharomyces cerevisiae RFC3* gene, an essential component of replication factor C. Proc. Natl. Acad. Sci. USA **91**: 868–872.
33. **Lipke, P. N., D. Wojciechowicz, and J. Kurjan.** 1989. *Agα1* is the structural gene for the *Saccharomyces cerevisiae* α-agglutinin, a cell surface glycoprotein involved in cell-cell interactions during mating. Mol. Cell. Biol. **9**:3155–3165.
34. **Lowry, O. H., N. J. Rosebrough, A. L. Farr, and R. J. Randall.** 1951. Protein measurement with the Folin phenol reagent. J. Biol. Chem. **193**:265–275.
35. **MacKay, V. L., S. K. Welch, M. Y. Insley, T. R. Manney, J. Holly, G. C. Saari, and M. L. Parker.** 1988. The *Saccharomyces cerevisiae BAR1* gene encodes an exported protein with homology to pepsin. Proc. Natl. Acad. Sci. USA **85**:55–59.
36. **Marsh, L., A. M. Neiman, and I. Herskowitz.** 1991. Signal transduction during pheromone response in yeast. Annu. Rev. Cell Biol. **7**:699–728.
37. **McCaffrey, G., F. J. Clay, K. Kelsay, and G. F. Sprague, Jr.** 1987. Identification and regulation of a gene required for cell fusion during mating of the yeast *Saccharomyces cerevisiae*. Mol. Cell. Biol. **7**:2680–2690.
38. **Meluh, P. B., and M. D. Rose.** 1990. *KAR3*, a kinesin-related gene required for yeast nuclear fusion. Cell **60**:1029–1041.
39. **Mikami, A., K. Imoto, T. Tanabe, T. Niidome, Y. Mori, H. Takeshima, S. Narumiya, and S. Numa.** 1989. Primary structure and functional expression of the cardiac dihydropyridine-sensitive calcium channel. Cell **340**:230–233.
40. **Nakamura, T., Y. Liu, D. Hirata, H. Namba, S. Harada, T. Hirokawa, and T. Miyakawa.** 1993. Protein phosphatase type 2B (calcineurin)-mediated, FK506-sensitive regulation of intracellular ions in yeast is an important determinant for adaptation to high salt stress conditions. EMBO. J. **12**:4063–4071.
41. **Ohsumi, Y., and Y. Anraku.** 1985. Specific induction of Ca^{2+} transport activity in *MATa* cells of *Saccharomyces cerevisiae* by a mating pheromone, α-factor. J. Biol. Chem. **260**:10482–10486.
42. **Prasad, K. R., and P. M. Rosoff.** 1992. Characterization of the energy-dependent, mating-factor activated Ca^{2+} influx in *Saccharomyces cerevisiae*. Cell Calcium **13**:615–626.
43. **Robinson, J. S., T. R. Graham, and S. D. Emr.** 1991. A putative zinc finger protein, *Saccharomyces cerevisiae* Vps18p, affects late Golgi functions required for vacuolar protein sorting and efficient α-factor prohormone maturation. Mol. Cell. Biol. **11**:5813–5824.
44. **Rose, M. D., and G. R. Fink.** 1987. *KAR1*, a gene required for

function of both intranuclear and extranuclear microtubules in yeast. Cell **48:**1047–1060.

45. **Rose, M. D., L. M. Misra, and J. P. Vogel.** 1989. *KAR2*, a karyogamy gene, is the yeast homolog of the mammalian BiP/GRP78 gene. Cell **57:**1211–1221.
46. **Rothstein, R.** 1991. Targeting, disruption, replacement, and allele rescue: integrative DNA transformation method in yeast. Methods Enzymol. **194:**281–301.
47. **Sambrook, J., E. F. Fritsch, and T. Maniatis.** 1989. Molecular cloning: a laboratory manual, 2nd ed. Cold Spring Harbor Laboratory Press, Cold Spring Harbor, N.Y.
48. **Sanger, F., S. Nicklen, and A. R. Coulson.** 1977. DNA sequencing with chain-terminating inhibitors. Proc. Natl. Acad. Sci. USA **74:**5463–5467.
49. **Scott, J. H., and R. Schekman.** 1980. Lyticase: endoglucanase and protease activities that act together in yeast cell lysis. J. Bacteriol. **142:**414–423.
50. **Serrano, R., B. C. Monk, J. M. Villalba, C. Montesinos, and E. W. Weiler.** 1993. Epitope mapping and accessibility of immunodominant regions of yeast plasma membrane H^+-ATPase. Eur. J. Biochem. **212:**737–744.
51. **Sherman, F., G. R. Fink, and J. B. Hicks.** 1986. Methods in yeast genetics. Cold Spring Harbor Laboratory, Cold Spring Harbor, N.Y.
52. **Sikorski, R. S., and P. Hieter.** 1989. A system of shuttle vectors and yeast host strains designed for efficient manipulation of DNA in *Saccharomyces cerevisiae*. Genetics **122:**19–27.
53. **Sprague, G. F., Jr., and I. Herskowitz.** 1981. Control of yeast cell type by the mating type locus. I. Identification and control of expression of the **a**-specific gene, *BAR1*. J. Mol. Biol. **153:**305–321.
54. **Sprague, G. F., Jr., and J. W. Thorner.** 1992. Pheromone response and signal transduction during the mating process of *Saccharomyces cerevisiae*, p. 657–744. *In* E. W. Jones, J. R. Pringle, and J. R. Broach (ed.), The molecular and cellular biology of the yeast *Saccharomyces*. Gene expression. Cold Spring Harbor Laboratory, Cold Spring Harbor, N.Y.
55. **Suzuki, K., and N. Yanagishima.** 1985. An alpha-mating-type specific defect in sexual agglutinability in the yeast *Saccharomyces cerevisiae*. Curr. Genet. **9:**185–189.
56. **Thorner, J.** 1981. Pheromonal regulation of development in *Saccharomyces cerevisiae*, p. 143–180. *In* E. W. Jones, J. N. Strathern, and J. R. Broach (ed.), The molecular biology of the yeast *Saccharomyces*. Life cycle and inheritance. Cold Spring Harbor Laboratory, Cold Spring Harbor, N.Y.
57. **Trueheart, J., J. D. Boeke, and G. R. Fink.** 1987. Two genes required for cell fusion during yeast conjugation: evidence for a pheromone-induced surface protein. Mol. Cell. Biol. **7:**2316–2328.
58. **Wilson, I. A., H. L. Niman, R. A. Houghten, A. R. Cherenson, M. L. Connolly, and R. A. Lerner.** 1984. The structure of an antigenic determinant in a protein. Cell **37:**767–778.
59. **Yoshihisa, T., and Y. Anraku.** 1989. Nucleotide sequence of *AMS1*, the structural gene of vacuolar α-mannosidase of *Saccharomyces cerevisiae*. Biochem. Biophys. Res. Commun. **163:**908–915.